Coordination Polymers

DOI: 10.1002/anie.201404306

Design of Superhydrophobic Porous Coordination Polymers through the Introduction of External Surface Corrugation by the Use of an Aromatic Hydrocarbon Building Unit**

*Koya Prabhakara Rao, Masakazu Higuchi, Kenji Sumida, Shuhei Furukawa, Jingui Duan, and Susumu Kitagawa**

Abstract: *We demonstrate a new approach to superhydrophobic porous coordination polymers by incorporating an anisotropic crystal morphology featuring a predominant surface that is highly corrugated and terminated by aromatic hydrocarbon moieties. The resulting low-energy surface provides particularly promising hydrophobic properties without the need for postsynthetic modifications or surface processing that would block the porosity of the framework. Consequently, hydrophobic organic molecules and water vapor are able to penetrate the surface and be densely accommodated within the pores, whereas bulk water is repelled as a result of the exterior surface corrugation derived from the aromatic surface groups. This study provides a new strategy for the design and development of superhydrophobic porous materials.*

Porous coordination polymers (PCPs), or metal–organic frameworks (MOFs), have emerged as potential materials for a variety of applications, such as gas storage,[1] separation,[2] and catalysis.[3] The ability to finely tune the physical and chemical properties of the pores within these materials represents a considerable advantage over other types of porous media, such as activated carbon materials and zeolites.[4] For applications that require the performance of the materials to be maintained in the presence of water vapor or liquid water, careful consideration of the stability profile is of importance, particularly if the material is to be recovered and reused in later cycles. Whereas many materials reported to date have limited direct applicability for real-world use owing to their propensity for degradation upon exposure to water,[5] materials which feature very strong metal–ligand bonds that are not readily hydrolyzed or which contain organic units bearing hydrophobic groups have been shown to have enhanced stability in this regard.[6] A related strategy of particular interest for promoting greater stability in liquid water would be to create a (super)hydrophobic external surface that does not permit the entry of water into the pores. This approach has been pursued predominantly by postsynthetic strategies in which hydrophobic groups, such as alkyl chains, are grafted to the surface of the PCP crystals following synthesis. Although this strategy can be effective in excluding water from the pores, the inherent porosity of the interior of the crystals also becomes largely inaccessible as a result of the steric bulk of the grafted groups. This effect is a crucial disadvantage in applications requiring the retention of porosity, such as the removal of organic compounds from aqueous media or gas separation under humid conditions.

An alternative strategy for providing highly hydrophobic exterior surfaces while retaining the internal porosity would be the generation of surface roughness on the nano-to-micrometer length scale. It is well-known that the texturing of a solid surface can significantly increase its hydrophobicity with respect to liquid water. For example, the contact angle of a water droplet on a flat solid terminated by $-CF_3$ groups is approximately 120°,[7] whereas it reaches values as high as 160–175° following the introduction of fractal roughness[8] or microtextures.[9] The highest contact-angle values are obtained when the roughened external surface is also a so-called "low-energy surface" consisting of alkyl or fluoroalkyl groups that interact very weakly with water and do not promote the efficient spreading of water droplets on the surface.[6d,e,h] Thus, in the context of PCPs, compounds featuring an anisotropic crystal morphology with a predominant surface that is both highly corrugated and terminated by aromatic hydrocarbon moieties, which would provide a low-energy surface (but to a lesser extent than alkyl or fluoroalkyl groups),[10] are expected to provide a high level of hydrophobicity without the need for postsynthetic modifications or surface processing of the type that would reduce (or

[*] Dr. K. P. Rao,[+] Dr. M. Higuchi, Dr. K. Sumida, Dr. S. Furukawa, Dr. J. Duan, Prof. S. Kitagawa
Institute for Integrated Cell-Material Sciences (iCeMS)
Kyoto University
Yoshida, Sakyo-ku, Kyoto 606-8501 (Japan)
E-mail: kitagawa@icems.kyoto-u.ac.jp
Dr. M. Higuchi
Japan Science and Technology Agency, PRESTO
4-1-8 Honcho, Kawaguchi, Saitama 332-0012 (Japan)
Prof. S. Kitagawa
Department of Synthetic Chemistry and Biological Chemistry, Graduate School of Engineering, Kyoto University
Katsura, Nishikyo-ku, Kyoto 615-8510 (Japan)
[+] Present address: Chemistry Division
Department of Sciences and Humanities, VFSTR University
Vadlamudi-522 213 (India)

[**] This research was supported by the Advanced Catalytic Transformation Program for Carbon Utilization (ACT-C), the PRESTO Program of the Japan Science and Technology Agency (JST), ENEOS Hydrogen Trust Fund, and MEXT Project for Developing Innovation Systems Regional Innovation Strategy Support Program Kyoto Next-Generation Energy System Creation Strategy (MEXT: the Ministry of Education, Culture, Sports, Science and Technology of Japan. The Institute for Integrated Cell-Material Sciences (iCeMS) is supported by the World Premier International Research Initiative (WPI).

Supporting information for this article is available on the WWW under http://dx.doi.org/10.1002/anie.201404306.

completely block) the inherent porosity of the framework. Herein, we report the synthesis and characterization of a PCP with external surface design (PESD), $[Zn_4(\mu_3\text{-}OH)_2(BTMB)_2(DMF)_3(MeOH)]\cdot(DMF)_2(MeOH)$ (**PESD-1**⊃Guest; see definition of BTMB below), which possesses an aromatic terminating surface that is highly corrugated on the nanometer length scale. This feature results in superhydrophobicity without the use of bulky alkyl or fluorinated organic groups and thus enables full accessibility of the pores to be preserved. Consequently, hydrophobic organic molecules are able to infiltrate the surface and be densely accommodated within the pores, whereas bulk water is repelled as a result of the exterior surface roughness derived from the aromatic surface. Such superhydrophobic materials could be suitable for a variety of technological applications,[11] such as coatings, paints, roof tiles, and fabrics.

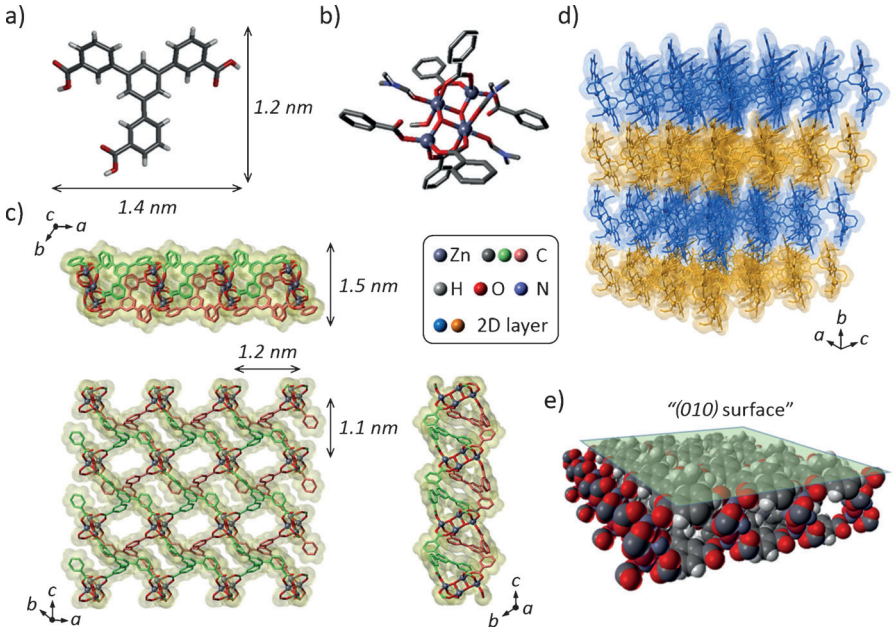

Figure 1. X-ray single-crystal structures showing a) 1,3,5-tris(3-carboxyphenyl)benzene (H_3BTMB, from "benzene-1,3,5-tris(*m*-benzoic acid)"), b) the coordination environment around a single $[Zn_4(\mu_3\text{-}OH)_2]^{6+}$ cluster, c) views of a 2D layer consisting of the clusters shown in (b) linked by $BMTB^{3-}$ linkers, d) the 3D stacking of individual 2D layers, and e) the structure of the (0*k*0) surface, which affords a low-energy surface. Hydrogen atoms and solvent molecules have been omitted for clarity in many structures.

The design of new PCPs requires careful initial selection of the organic bridging unit owing to its significant influence over the chemical and structural properties of the resultant network. Low-symmetry linkers[12] with a molecular diameter on the order of approximately 1–2 nm are of particular interest owing to their potential for forming highly anisotropic networks that have dominant crystal planes featuring a large contribution of organic surfaces with nanoscale periodicity. Smaller organic units frequently form networks featuring periodicities that are on the order of several angstroms (< 1 nm), which would result in surface corrugations that are constructed by phenyl moieties and are fine enough to greatly impact the contact surface with liquid water. As such, 1,3,5-tris(3-carboxyphenyl)benzene[13] (H_3BTMB, Figure 1a; see also Figure S1) is an ideal candidate owing to its low symmetry and molecular size. We therefore screened its reactivity with a variety of transition-metal ions.

A reaction of H_3BTMB with $Zn(NO_3)_2\cdot4H_2O$ in the solvent mixture DMF/MeOH/H_2O (2:1:1) at 100 °C resulted in colorless, block-shaped crystals (Scheme 1).[14] Single-crystal X-ray analysis of the solvated framework (**PESD-1**⊃Guest; Figure 1b–e; see also Table S1 and Figures S2 and S7 in the Supporting Information) subsequently revealed a two-dimensional layered structure (Figure 1c) possessing two types of 1D channels along the *b* axis. Each of the individual layers comprise rhombus-shaped $[Zn_4(\mu_3\text{-}OH)_2]^{6+}$ tetranuclear clusters[15] that are mutually connected through the $BTMB^{3-}$ ligands to form an (8,6) net. As shown in Figure 1b, the $[Zn_4(\mu_3\text{-}OH)_2]^{6+}$ clusters each comprise two octahedral and two tetrahedral Zn^{2+} ions, and two μ_3-hydroxy moieties (OH^-) that are located within three-atom mean

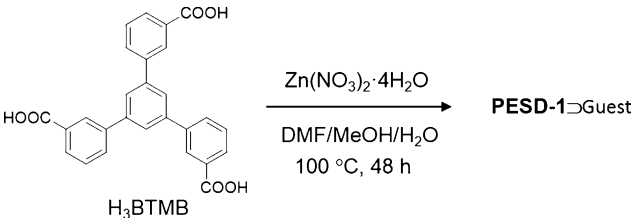

Scheme 1. Synthesis of **PESD-1**⊃Guest. DMF = *N*,*N*-dimethylformamide.

planes formed by the metal centers. The octahedral Zn^{2+} centers are bound to oxygen donors of three different carboxylate groups, both OH^- fragments, and a solvent molecule, whereas the tetrahedral Zn^{2+} centers are coordinated by oxygen atoms of three carboxylate groups and just one of the OH^- groups. Although the individual layers are relatively dense, the voids formed between layers are large enough to accommodate guest molecules. Indeed, CO_2-adsorption experiments performed at 195 K (see Figure S15) revealed a type-I isotherm, which is characteristic of a microporous solid with permanent porosity.[16] The Brunauer–Emmett–Teller (BET) surface area evaluated from the CO_2-adsorption data is 295 m^2g^{-1}, and the Langmuir surface area was calculated to be 570 m^2g^{-1}, thus indicating that **PESD-1** has modest porosity available for guest inclusion.

The highly anisotropic morphology of the single crystals of **PESD-1**⊃Guest enabled face indexing to be performed and thus elucidation of the structural and chemical nature of the surface of the crystals. Face-index measurement identified

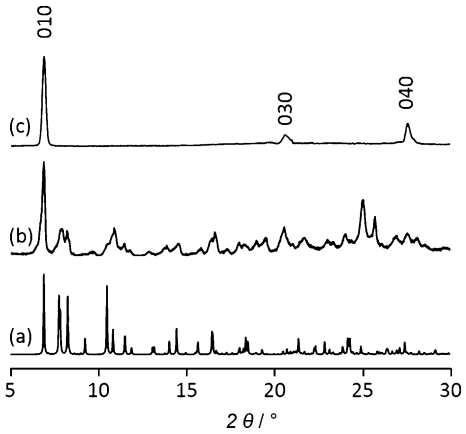

Figure 2. XRPD patterns of **PESD-1**⊃Guest: a) simulated pattern; b) powder; c) single crystal (flake shape).

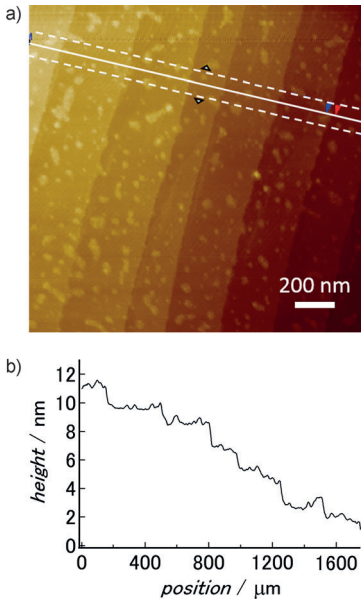

Figure 3. a) AFM image of the (010) surface of **PESD-1**⊃Guest. b) Averaged topographic profile of the portion of the surface enclosed within the dotted lines in (a). The AFM topographic image of the (010) surface exhibits terrace structures with widths in the range of 100–400 nm. The stepped structure displays discrete displacements of approximately 1.5 nm per step, which corresponds to the length of the *b* axis (1.41 nm), and reveals the flat nature of the (010) surface at the nanoscale (as observed previously for other PCPs/MOFs[17]).

the most dominant surface at the crystal surface as the (010) surface (Figure 1e), in close agreement with X-ray powder-diffraction data collected on (flake-shaped) single crystals of **PESD-1**, which exhibited a strong preferential orientation along the [0*k*0] direction (Figure 2). Calculation of the Bravais–Friedel–Donnay–Harker (BFDH) crystal morphology on single-crystal X-ray data of **PESD-1**⊃Guest (see Figure S2b) indicated that the (010) surface possesses nanoscaled corrugation (with a periodicity of 1.2×1.1 nm^2 in the *ac* plane) arising from the aromatic portions of the $BMTB^{3-}$ linker (Figure 1e).[10] To obtain information about the nano-to-micrometer-scale roughness of the (010) surface, we carried out atomic force microscopy (AFM) and field-emission scanning electron microscopy (FESEM). Both the AFM (Figure 3) and the FESEM (see Figure S12) images revealed that the (010) surface is flat over the nano-to-micrometer length scale. Thus, no roughness in the range of several nanometers to several micrometers was observed, although roughness beyond several hundred micrometers was observed (see below).

To examine its hydrophobic properties, we carried out contact-angle measurements on four different states of the material: single crystals, as-synthesized powders, degassed powders, and a pressed pellet (Figure 4 and Table 1; see also Figures S11 and S13). For the (flake-shaped) single-crystal form of **PESD-1**⊃Guest, the contact angle was observed to be more than 150°, and the roll-off angle was less than 10°, which is characteristic of a superhydrophobic solid (Figure 4a). We also studied the effect of the presence of the guest on the hydrophobicity by performing contact-angle experiments on both as-synthesized powders of **PESD-1**⊃Guest and degassed powders of **PESD-1**. Both powders also displayed super-

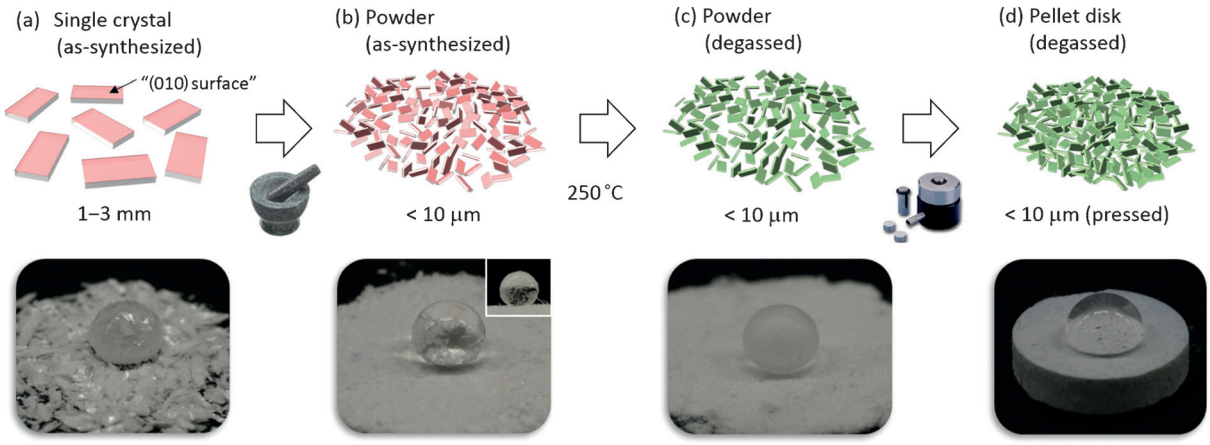

Figure 4. Schematic representation of **PESD-1** in four states, and pictures of a water droplet on corresponding **PESD-1** samples. Pink objects are as-synthesized forms, and green objects are degassed forms.

Table 1: Contact angle for several states of **PESD-1** and other PCPs/MOFs.

PCP/MOF	Surface modification		Form investigated	As-synthesized (A) or degassed (D)	Contact angle [°]	Ref.
	Type	Structure of organic linker				
PESD-1	aromatic ring	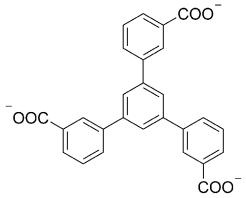	single crystal	A	>150[a]	
			powder	A	>150[a]	
			powder	D	>150[a]	
			pellet disk (5 MPa)	D	ca. 110	
MIL-53(Al)-AM4	alkyl chain (C_4)	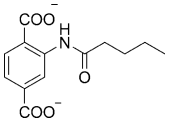	powder	–	>150[b]	[6e]
MIL-53(Al)-AM6	alkyl chain (C_6)	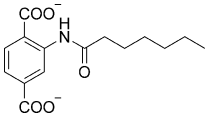	powder	–	>150[b]	[6e]
SIM-2(C12)/Al_2O_3	alkyl chain (C_{12})	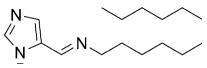	film on Al_2O_3 support	–	>150[c]	[6h]
MOFF-1	fluorinated aromatic ring	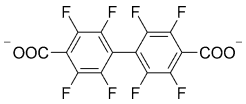	pressed crystals	D	108 ± 2[d]	[6b]
MOFF-2	fluorinated aromatic ring	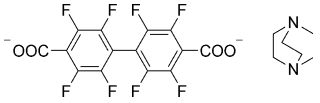	pressed crystals	D	151 ± 1[d]	[6b]
MOFF-3	fluorinated aromatic ring	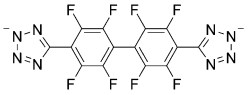	pressed crystals	D	135 ± 2[e]	[6b]

[a] As for conventional superhydrophobic nanomaterials and thin films, it is difficult to make hard and flat surfaces in the case of powder samples of PCPs/MOFs. The contact angle of the **PESD-1** powder sample shown in Figure 4 is estimated to be 152°. [b] Water droplets were observed to rapidly roll off of the surface of the material. [c] The contact angle was judged from the picture in Ref. [6h]. [d] The material was dried in a vacuum oven (120 °C, 24 h). [e] The material was dried with supercritical CO_2.

hydrophobicity (Figure 4b,c), thus indicating that this property of **PESD-1** is not affected by the presence of solvent within the pores. These results clearly indicate that the (010) surface of **PESD-1**⊃Guest exhibits superhydrophobicity without the grafting of hydrophobic alkyl chains to the surface[6d,e,h] or the use of a fluorinated aromatic ligand,[6b] presumably because the surface corrugation of the (010) surface remains unchanged between the as-synthesized and degassed forms, as evidenced by the single-crystal structures of the two forms (Figure 1c and Figure S3c). As shown by FESEM (see Figure S12), the crystal size of both the as-synthesized and evacuated forms is in the range of 100–300 μm, which is a size range in which an additional level of corrugation exists over longer length scales (of a few hundred micrometers) in the powder phase. Thus, the powder states also exhibit superhydrophobicity in spite of nonoriented crystal surfaces. Thus, the (010) surface corrugation, as elucidated by single-crystal analysis, intrinsically plays a key role in the superhydrophobicity of the material. This effect is accompanied by a contribution from microscaled roughness, as observed by FESEM experiments, thus leading to a hierarchical structure that exhibits superhydrophobicity.[18] In the case of the pressed pellet form, the contact angle measured was decreased as a result of the significantly smoother surface owing to the compressive force of 5 MPa (Figure 4d). The fact that the application of pressure, and hence a decrease in the level of microscaled roughness, is of detriment to the hydrophobicity (contact angle: ca. 110°) provides further evidence that the hierarchical structure in the powder phase is responsible for the superhydrophobicity.

All PCPs bearing grafted aromatic ligands with alkyl chains (MIL-53(Al)-AM4, MIL-53(Al)-AM6, and SIM-2-(C12)) exhibit a contact angle of over 150° as a result of the presence of surface roughness and low-energy surfaces (Table 1). On the other hand, among PCPs that possess fluorinated aromatic ligands, only MOFF-2 exhibits superhydrophobicity, with a contact angle of approximately (151 ± 1)°, and the other members of the series, MOFF-1 and MOFF-3, are hydrophobic materials with contact angles of (108 ± 2) and (135 ± 2)°, respectively. As compared to these hydrophobic and superhydrophobic PCPs prepared by the grafting of alkyl groups or the use of fluorinated aromatic

ligands, **PESD-1** is distinctive in possessing superhydrophobicity derived from nanoscaled corrugation introduced by the use of an aromatic hydrocarbon bridging unit. To our knowledge, superhydrophobicity has not been achieved previously by the fusion of a low-energy surface with nanoscaled corrugation due to an aromatic hydrocarbon ligand without the use of bulky alkyl or fluoroalkyl groups.

The superhydrophobic PCPs reported to date exhibit very low water-vapor-adsorption capacities at high relative humidities. Water-adsorption-isotherm experiments on **PESD-1** at 298 K (see Figure S16) showed unusual adsorption behavior, with two steps at 0.27 and 2.3 kPa in the adsorption isotherm and (in contrast to other superhydrophobic PCPs) no steps in the desorption isotherm. The isotherm clearly indicates that interior pore surfaces are in fact hydrophilic and that only the exterior crystal surface of **PESD-1** exhibits superhydrophobicity toward liquid water (similar to a lotus leaf[19]). This phenomenon further supports the hypothesis that the superhydrophobicity of **PESD-1** originates from surface structural roughness rather than from chemical features of the surface. To understand the structural flexibility during the adsorption, we carried out in situ water-isotherm–XRPD measurements on **PESD-1** (see Figure S17), because 2D layered PCPs often show flexibility during sorption processes. The isotherm–XRPD patterns clearly indicated that **PESD-1** is flexible. A small diffraction from the 010 Bragg position observed at a pressure of 0.20 kPa in the water-isotherm–XRPD pattern is similar to the peak observed for a degassed sample in an open atmosphere (see Figure S17).

We also investigated the sorption ability of **PESD-1** for six-membered-ring organic solvents. Sorption isotherms were measured for benzene, toluene, and cyclohexane at 298 K (Figure 5). The adsorption isotherms for benzene and toluene showed a gate-opening profile, whereas cyclohexane was excluded from the pores. These results indicated size selectivity of **PESD-1** toward guest molecules, but also the flexibility of the framework.[20] The experiments clearly demonstrate that **PESD-1** can accommodate a variety of aromatic solvents. By taking advantage of the superhydrophobic surfaces in the powder state (or hydrophobic surfaces in the pellet-disk form) of **PESD-1**, while retaining the porosity of the parent framework, we carried out the experiments to demonstrate the removal of organic solvents from a water surface. A pellet of **PESD-1** was placed within a mixture consisting of an organic solvent and water. Remarkably, owing to its superhydrophobicity, the pellet floated on the water surface without breakage, and consequently selectively removed the organic solvent from the water (see Figure S19 and movie file 1 in the Supporting Information). The powder, which is intrinsically water-repellent (see Figure S23), also selectively adsorbed organic solvents without decomposing, despite its immersion in liquid water (see the Supporting Information for details and movies), thus further reinforcing the utility of the material.

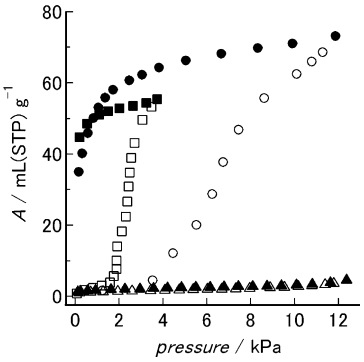

Figure 5. Adsorption isotherms of **PESD-1** recorded for benzene (circles), toluene (squares), and cyclohexane (triangles) at 298 K. Filled and open symbols represent adsorption and desorption data, respectively.

In conclusion, we have successfully synthesized a new PCP with superhydrophobic surfaces as a result of nanoscaled corrugation of a predominantly organic surface at the crystal interface, without the use of alkylation or fluorination. The material adsorbs water vapor despite its superhydrophobicity, whereas its ability to repel liquid water enables this PCP to adsorb organic solvents dispersed on bulk water without decomposition of the framework. These results provide a roadmap for the design and synthesis of novel porous materials with superhydrophobic surfaces on the basis of external surface design at the nanoscale.

Received: April 15, 2014
Published online: June 27, 2014

Keywords: contact angles · coordination polymers · materials science · selective sorption · superhydrophobicity

[1] a) M. Kondo, T. Yoshitomi, K. Seki, H. Matsuzaka, S. Kitagawa, *Angew. Chem.* **1997**, *109*, 1844 – 1846; *Angew. Chem. Int. Ed. Engl.* **1997**, *36*, 1725 – 1727; b) G. Férey, C. Mellot-Draznieks, C. Serre, F. Millange, J. Dutour, S. Surblé, I. Margiolaki, *Science* **2005**, *309*, 2040 – 2042.

[2] a) L. Pan, D. H. Olson, L. R. Ciemnolonski, R. Heddy, J. Li, *Angew. Chem.* **2006**, *118*, 632 – 635; *Angew. Chem. Int. Ed.* **2006**, *45*, 616 – 619; b) J. R. Li, R. J. Kuppler, H. C. Zhou, *Chem. Soc. Rev.* **2009**, *38*, 1477 – 1504.

[3] a) J. S. Seo, D. Whang, H. Lee, S. I. Jun, J. Oh, Y. J. Jeon, K. Kim, *Nature* **2000**, *404*, 982 – 986; b) C. D. Wu, A. Hu, L. Zhang, W. B. Lin, *J Am Chem. Soc* **2005**, *127*, 8940 – 8941; c) S. H. Cho, B. Q. Ma, S. T. Nguyen, J. T. Hupp, T. E. Albrecht-Schmitt, *Chem. Commun.* **2006**, 2563 – 2565; d) S. Hasegawa, S. Horike, R. Matsuda, S. Furukawa, K. Mochizuki, Y. Kinoshita, S. Kitagawa, *J. Am. Chem. Soc.* **2007**, *129*, 2607 – 2614.

[4] a) S. Horike, M. Dinca, K. Tamaki, J. R. Long, *J. Am. Chem. Soc.* **2008**, *130*, 5854 – 5855; b) M. Higuchi, K. Nakamura, S. Horike, Y. Hijikata, N. Yanai, T. Fukushima, J. Kim, K. Kato, M. Takata, D. Watanabe, S. Oshima, S. Kitagawa, *Angew. Chem.* **2012**, *124*, 8494 – 8497; *Angew. Chem. Int. Ed.* **2012**, *51*, 8369 – 8372; c) M. Fujita, Y. J. Kwon, S. Washizu, K. Ogura, *J. Am. Chem. Soc.* **1994**, *116*, 1151 – 1152.

[5] a) S. Hausdorf, J. Wagler, R. Moßig, F. O. R. L. Mertens, *J. Phys. Chem. A* **2008**, *112*, 7567 – 7576; b) S. S. Kaye, A. Dailly, O. M. Yaghi, J. R. Long, *J. Am. Chem. Soc.* **2007**, *129*, 14176 – 14177; c) H. Furukawa, N. Ko, Y. B. Go, N. Aratani, S. B. Choi, E. Choi, A. O. Yazaydin, R. Q. Snurr, M. O'Keeffe, J. Kim, O. M. Yaghi, *Science* **2010**, *329*, 424 – 428; d) H. K. Chae, D. Y. Siberio-Pérez, J. Kim, Y. Go, M. Eddaoudi, A. J. Matzger, M. O'Keeffe, O. M. Yaghi, *Nature* **2004**, *427*, 523 – 527.

[6] a) V. Colombo, S. Galli, H. J. Choi, G. D. Han, A. Maspero, G. Palmisano, N. Masciocchi, J. R. Long, *Chem. Sci.* **2011**, *2*, 1311 – 1319; b) T.-H. Chen, I. Popov, O. Zenasni, O. Daugulis, O. S. Miljanic, *Chem. Commun.* **2013**, *49*, 6846 – 6848; c) I. J. Kang, N. A. Khan, E. Haque, S. H. Jhung, *Chem. Eur. J.* **2011**, *17*, 6437 – 6442; d) Z. Q. Wang, S. M. Cohen, *Chem. Soc. Rev.* **2009**, *38*, 1315 – 1329; e) J. G. Nguyen, S. M. Cohen, *J. Am. Chem. Soc.* **2010**, *132*, 4560 – 4561; f) C. Yang, U. Kaipa, Q. Z. Mather, X. P. Wang, V. Nesterov, A. F. Venero, M. A. Omary, *J. Am. Chem. Soc.* **2011**, *133*, 18094 – 18097; g) C. Serre, *Angew. Chem.* **2012**, *124*, 6152 – 6154; *Angew. Chem. Int. Ed.* **2012**, *51*, 6048 – 6050; h) S. Aguado, J. Canivet, D. Farrusseng, *J. Mater. Chem.* **2011**, *21*, 7582 – 7588.

[7] a) T. Nishino, M. Meguro, K. Nakamae, M. Matsushita, Y. Ueda, *Langmuir* **1999**, *15*, 4321 – 4323; b) S. R. Coulson, I. Woodward, J. P. S. Badyal, S. A. Brewer, C. Willis, *J. Phys. Chem. B* **2000**, *104*, 8836 – 8840.

[8] a) T. Onda, S. Shibuichi, N. Satoh, K. Tsujii, *Langmuir* **1996**, *12*, 2125 – 2127; b) S. Shibuichi, T. Onda, N. Satoh, K. Tsujii, *J. Phys. Chem.* **1996**, *100*, 19512 – 19517.

[9] a) S. Herminghaus, *Europhys. Lett.* **2000**, *52*, 165 – 170; b) D. Öner, T. J. McCarthy, *Langmuir* **2000**, *16*, 7777 – 7782.

[10] E. G. Shafrin, W. A. Zisman, *J. Phys. Chem.* **1960**, *64*, 519 – 524.

[11] a) D. Ehre, E. Layert, M. Lahav, I. Lubomirsky, *Science* **2010**, *327*, 672 – 675; b) L. Mishchenko, M. Khan, J. Aizenberg, B. D. Hatton, *Adv. Funct. Mater.* **2013**, *23*, 4577 – 4584; c) A. D. Stroock, S. K. W. Dertinger, A. Ajdari, I. Mezic, H. A. Stone, G. M. Whitesides, *Science* **2002**, *295*, 647 – 651; d) J.-M. Nam, C. S. Thaxton, C. A. Mirkin, *Science* **2003**, *301*, 1884 – 1886; e) S. Minko, M. Müller, M. Motornov, M. Nitschke, K. Grundke, M. Stamm, *J. Am. Chem. Soc.* **2003**, *125*, 3896 – 3900; f) O. Shekhah, J. Liu, R. A. Fischer, C. Wöll, *Chem. Soc. Rev.* **2009**, *38*, 1477 – 1504.

[12] J. K. Schnobrich, O. Lebel, K. A. Cychosz, A. Dailly, A. G. Wong-Foy, A. J. Matzger, *J. Am. Chem. Soc.* **2010**, *132*, 13941 – 13948.

[13] Y. B. He, Z. Bian, C. Q. Kang, Y. Q. Cheng, L. X. Gao, *Tetrahedron* **2010**, *66*, 3553 – 3563.

[14] CCDC 977651 (**PESD-1**⊃Guest), 977650 (H_3BTMB ligand), and 977652, 977653 (**PESD-1**⊃Guest1&Guest2) contain the supplementary crystallographic data for this paper. These data can be obtained free of charge from The Cambridge Crystallographic Data Centre via www.ccdc.cam.ac.uk/data_request/cif.

[15] The OH^- groups are assigned as such for charge compensation, evidence for which was provided by FTIR spectroscopy (broad peak of an O–H stretch at 3615 cm^{-1}; see Figure S6): F. Vermoortele, R. Ameloot, A. Vimont, C. Serre, D. De Vos, *Chem. Commun.* **2011**, *47*, 1521 – 1523.

[16] This material does not adsorb N_2 at 77 K, presumably because the minor structural rearrangement that occurs upon adsorption is blocked at low temperatures for adsorbates that are not strongly bound.

[17] M. Kondo, S. Furukawa, K. Hirai, S. Kitagawa, *Angew. Chem.* **2010**, *122*, 5455 – 5458; *Angew. Chem. Int. Ed.* **2010**, *49*, 5327 – 5330.

[18] B. Bhushan, Y. C. Jung, K. Koch, *Philos. Trans. R. Soc. London Ser. A* **2009**, *367*, 1631 – 1672.

[19] A. B. D. Cassie, S. Baxter, *Trans. Faraday Soc.* **1944**, *40*, 546 – 550.

[20] S. Shimomura, S. Horike, R. Matsuda, S. Kitagawa, *J. Am. Chem. Soc.* **2007**, *129*, 10990 – 10991.

